

**Integrin-engagement increases histone H3 acetylation and reduces histone H1
association with DNA in murine lung endothelial cells**

Jane L. Rose, Hong Huang, Scott F. Wray and Dale G. Hoyt

*Division of Pharmacology, The Ohio State University College of Pharmacy, and The Dorothy M.
Davis Heart and Lung Research Institute, Columbus, OH 43210*

Running Title: Integrin regulation of histone-DNA interactions

Keywords: acetylation, chromatin, endothelium, histone, integrin, lung, PARP-1

*Author for correspondence: Dale G. Hoyt, Ph.D.

Division of Pharmacology, The Ohio State University College of Pharmacy, 500 West
Twelfth Avenue, Columbus, OH, USA, 43210.

E-mail address: hoyt.27@osu.edu

Tel. (614) 292-6245; FAX (614) 292-9083

Text Pages: 26

Figures: 9

Tables: 0

Abstract: 229 words

Introduction: 513 words

Discussion: 866 words

Reference: 26

Chromatin Immunoprecipitation (ChIP); Deoxyribonuclease I, DNase I; Dulbecco's minimum essential medium, DMEM; ethylenediamine tetraacetic acid, EDTA; fetal bovine serum, FBS; horseradish peroxidase, HRP; inducible nitric oxide synthase, (iNOS); intercellular cell adhesion molecule-1, ICAM-1; in situ nick translation, ISNT; mouse lung endothelial cells, MLEC; phosphate-buffered saline, PBS; poly(ADP-ribose) polymerase-1, PARP-1; polymerase chain reaction, PCR; relative fluorescence units, RFU; sodium dodecylsulfate, SDS; tris-buffered saline buffer, TTBS; vascular cell adhesion molecule-1, VCAM-1.

Abstract

Engagement of integrin cell adhesion receptors in mouse lung endothelial cells induces global sensitivity of DNA to nuclease digestion reflecting alterations in chromatin structure. These structural changes may contribute to the anti-genotoxic effects of integrin-engagement in lung endothelium. Since histone acetylation and poly(ADP-ribosyl)ation modulate chromatin structure, we investigated the effects of $\beta 1$ integrin-engagement with antibody on these post-translational modifications, and the presence of histones at discrete DNA sequences in the mouse lung endothelial cell genome using chromatin immunoprecipitation. Integrin-engagement increased acetylation of core histone H3. The presence of acetylated histone H3 at intercellular and vascular cell adhesion molecule-1 (ICAM-1 and VCAM-1) promoters and a non-promoter sequence was also increased. As with integrin-engagement, the histone deacetylase inhibitor, trichostatin A, caused global hypersensitivity of DNA to nuclease digestion, induced acetylation of histone H3 and its co-immunoprecipitation with VCAM-1 and ICAM-1 promoters and non-promoter DNA. In contrast to acetyl-histone H3, the association of linker histone H1 with specific DNA sequences was either reduced or unaffected by integrin-engagement and trichostatin A. While integrin-engagement and trichostatin A treatment did not affect histone H1 poly(ADP-ribosyl)ation, deletion of PARP-1 increased core histone H3 acetylation, and increased its level at the iNOS promoter, while decreasing the amount of histone H1. The results suggest that integrin-engagement, as well as trichostatin A and PARP-1 deletion, regulate chromatin structure via core histone H3 acetylation and reduced linker histone H1-DNA association.

Integrins are a family of heterodimeric cell surface receptors, comprised of $\alpha\beta$ subunits that mediate adhesion of cells to each other, extracellular matrix and other ligands. Integrins mediate signal transduction, and antibodies to specific subunits promote endothelial survival (Aplin et al., 1998; Meredith et al., 1993). Integrin signaling modulates DNA damage and anti-cancer drug action in various cell types (Buckley et al., 1999; Hazlehurst et al., 2001). Engagement of $\beta 1$ integrins with antibodies or peptide ligands inhibited acute DNA strand breakage caused by bleomycin (BLM) in mouse lung endothelial cells (MLEC) (Hoyt et al., 1997; Jones et al., 2001). Integrins also inhibit DNA strand breaks caused by bacterial endotoxin and the topoisomerase inhibitor, etoposide. This ability to inhibit DNA damage caused by numerous agents might be due to a common mechanism, such as an alteration in the nucleus or stimulation of DNA repair (Hoyt et al., 1996a; Hoyt et al., 1996b). Engagement of $\beta 1$ integrins indeed alters MLEC chromatin structure as indicated by an induction of global hypersensitivity of DNA to exogenous nucleases (Huang et al., 2003; Jones et al., 2001).

DNA digestion by nucleases is restricted by DNA-protein interactions in chromatin. Chromatin includes nuclear DNA organized in compact packages with proteins. The fundamental repeating unit of chromatin is the nucleosome which contains ~146-165 bp of DNA wrapped around histone proteins. The nucleosome consists of two each of the core histones H2A, H2B, H3 and H4. Linker histone H1 binds nucleosomes where the coil of DNA enters and exits the core particle, and attaches to DNA between nucleosomes offering further stabilization of the chromatin fibers (Hansen, 2002).

Chromatin structure is regulated by post-translational modifications of histones, and through chromatin remodeling complexes. Modifications of histones include acetylation, poly(ADP-ribosyl)ation, methylation, phosphorylation, ubiquitination and biotinylation (Hansen, 2002). Acetylation of core histones and poly(ADP-ribosyl)ation of linker histone enhance

digestibility of cellular DNA with nucleases (Perez-Lamigueiro and Alvarez-Gonzalez, 2004; Simpson, 1978).

Electrostatic effects of acetylation and poly(ADP-ribosyl)ation alter histone-DNA and – protein interactions in the nucleus, contributing to nuclease hypersensitivity. Acetylation of N-terminal tails of core histones neutralizes positive charge on lysines and disrupts interaction with negative phosphates in the backbone of DNA (Hansen, 2002). Poly(ADP-ribosyl)ation, largely mediated by poly (ADP-ribose) polymerase-1 (PARP-1), occurs mainly on linker histone H1. Negatively charged ADP-ribose polymers interact poorly with anionic DNA, increasing accessibility of proteins to DNA (Ame et al., 2004; D'Amours et al., 1999). These post-translational modifications may contribute to integrin-mediated alterations in chromatin.

Since acetylation and poly(ADP-ribosyl)ation regulate histone interactions with DNA and other proteins, we hypothesized that integrin-mediated nuclease hypersensitivity is due to one or both of these histone modifications. Integrin actions on acetylation of core histone H3 and poly(ADP-ribosyl)ation of linker histone H1 were measured and compared with the effect of raising histone acetylation with the histone deacetylase inhibitor, trichostatin A, and with PARP-1 knockout. Co-localization of these histones with specific DNA sequences in the genome of live cells was assessed by chromatin immunoprecipitation. The results suggest that integrin-engagement, trichostatin A and PARP-1 knockout each increase histone H3 acetylation and alter the association of histone H1 with DNA.

Materials and Methods

Reagents. Endothelial cell growth supplement, heparin, phenylmethanesulfonyl fluoride, goat anti-rat IgG, Phenol-chloroform-iso amyl alcohol and Bradford reagent were purchased from Sigma Chemical Co. (St Louis, MO). Fetal bovine serum was purchased from Hyclone Laboratories, Logan, UT. Rat anti-mouse β 1 Integrin antibody was from PharMingen (San Diego, CA). Mouse anti-histone H1, rabbit anti-histone H3 and rabbit anti-acetyl lysine 9 and 14 histone H3 were purchased from Upstate Biotechnologies Inc. (Charlottesville, VA). Rabbit anti-poly(ADP-ribose) was obtained from Biomol Research Laboratories, Inc. (Plymouth Meeting, PA). Mouse anti-PARP-1 C2-10 antibody was obtained from Trevigen Inc. (Gaithersburg, MD). Horseradish peroxidase (HRP)-conjugated goat anti-mouse and goat anti-rabbit were from Jackson Immunoresearch Laboratories, Inc. (West Grove, PA). Gamma Bind Plus Sepharose was from Amersham Biosciences (Uppsala, Sweden). Bovine serum albumin and Digoxigenin-11-dUTP was purchased from Roche Applied Science (Indianapolis, IN). DNA polymerase I was from New England Biolabs (Beverly, MA). Salmon sperm DNA, Proteinase K, deoxynucleotides, Platinum Taq DNA polymerase, Deoxyribonuclease I (DNase I), and trypsin was purchased from Invitrogen (Carlsbad, CA). Tris-base, sodium chloride, ethylenediamine tetraacetic acid (EDTA), Na_3VO_4 , NaF, Tween 20, formaldehyde, sodium dodecyl sulfate (SDS), agarose and ethidium bromide were from Fisher Scientific (Fair Lawn, NJ). Triton X-100 was purchased from Pierce (Rockford, IL).

Cell Culture. Murine lung microvascular endothelial cells (MLEC) were isolated from wild-type (+/+) and PARP-1 knockout (-/-) mice as described previously (Jones et al., 2001).

Treatment of Cells. Integrin-engagement with anti- β 1 Integrin antibody was performed as previously described (Hoyt et al., 1996a; Hoyt et al., 1996b). PARP-1 +/+ and -/- MLEC were

plated onto 75 cm² flasks and 24 hours later rinsed once with phosphate-buffered saline (PBS) and treated with 0 or 1 µg anti-β1 Integrin antibody/ml for 1 hr at 37°C. Goat anti-rat IgG was added to all flasks for another 4 hr of incubation at 37°C.

Cell Lysis. MLEC were washed 3 times with ice-cold PBS and lysed with lysis buffer containing 1% triton X-100, 50 mM Tris pH 7.5, 150 mM NaCl, 5 mM EDTA, 0.5 mM Na₃VO₄, 50 mM NaF, 10 µg/ml aprotinin, 10 µg/ml leupeptin, 10 µg/ml pepstatin A and 1 mM phenylmethylsulfonyl fluoride. Extracts were sonicated and protein concentration was determined by the Bradford assay.

Immunoprecipitation. For immunoprecipitation of histone H1, 200 µg of protein was incubated with 2 µg of anti-histone H1 antibody overnight at 4°C. 30% slurry of Protein G Sepharose was added to each sample and rocked gently at 4°C for another 1 hr. The antibody-antigen-sepharose pellet was washed 3 times in ice-cold lysis buffer and 2 times in 10 mM Tris pH 7.4. The washed pellet was reconstituted in protein loading buffer (62.5 mM Tris pH 6.8, 10% glycerol, 2% SDS, 5% β-mercaptoethanol and 0.003% bromphenol blue) and heated for 10 min at 95°C. Proteins were separated on a 4-20% Tris-glycine polyacrylamide gel.

Total Protein Preparation. For total protein analysis, 10 µg of protein was incubated with protein loading buffer and incubated for 10 min at 95°C. Proteins were separated on 4-20% Tris-glycine polyacrylamide gels.

Immunoblotting. After transfer, the blots were blocked with 3% non-fat dry milk in Tris-buffered saline buffer and Tween 20 (0.1% Tween 20, 10 mM Tris, pH 7.5 and 150 mM NaCl, TTBS) and probed with primary antibody for 1 hr at room temperature. After blots were washed,

appropriate HRP-conjugated secondary antibody was added and incubated for 1 hr. Proteins were visualized using enhanced chemiluminescent system and captured on X-ray film.

Chromatin Immunoprecipitation. After treatment, MLEC were fixed, by addition of formaldehyde to a concentration of 1% directly in the culture medium, for 10 minutes at 37°C. Cells were washed 3 times with PBS and scraped in ice-cold collecting buffer (PBS with 10 µg/ml leupeptin, 10 µg/ml aprotinin, 10µg/ml pepstatin A and 1 mM phenylmethanesulfonyl fluoride). Collected cells were centrifuged at 2000 rpm for 4 minutes at 4°C. Pellets were resuspended in ice-cold lysis buffer (1% SDS, 10 mM EDTA and 50 mM Tris pH 8.1) and incubated on ice for 10 minutes. Chromatin was sheared to 1 kilo-base fragments by sonication (4 pulses, 20 s per pulse, at one-sixth maximum power) followed by addition of dilution buffer (0.01% SDS, 1.1% Triton X-100, 1.2 mM EDTA, 16.7 mM Tris pH 8.1, 167 mM NaCl). Immunoprecipitation of target histone protein was performed with the addition of 10 µg anti-Histone H1 or 10 µg anti-acetyl histone H3 (Lys 9 and 14) with gentle rocking overnight at 4°C. Immune complexes were collected for 1 hour on Gamma Bind Plus Sepharose with 20 µg/ml salmon sperm DNA. Immune complexes were sequentially washed for 4 minutes on ice with elution buffer A (0.1% SDS, 2 mM EDTA, 20 mM Tris pH 8, 150 mM NaCl and 1% Triton X-100), elution buffer B (0.1% SDS, 2 mM EDTA, 20 mM Tris pH 8, 500 mM NaCl and 1% Triton X-100), elution buffer C (0.25 M LiCl, 1% NP-40, 1 mM EDTA, 10 mM Tris pH 8 and 1% sodium deoxycholate) and two washes with 10 mM Tris/1 mM EDTA (TE), pH 8. Immune complexes were eluted with 1% SDS in 0.1 M NaHCO₃ and incubated at 65°C overnight to reverse DNA-protein crosslinks. Following proteinase K digestion (20 µg, 1 hour, 45°C) DNA was recovered with phenol-chloroform-iso amyl alcohol extraction and precipitated in ethanol. DNA was resuspended in 13.5 µl TE and serially diluted to 1/12, 1/24, 1/48 and 1/96 of immunoprecipitated DNA for polymerase chain reactions (PCR) used to detect the relative level of specific DNA sequences

recovered with the immunoprecipitated protein. Input samples (1% of volume following sonication) were reverse cross-linked and processed in the same way as immunoprecipitated DNA. The following promoter specific primers were used. INOS: sense 5'-CAACTATTGAGGCCACACAC-3'; antisense 5'-AACCAGTGACACTGTGTCC-3'; 1133 bp product. VCAM-1: sense 5'- CATTCTGCATCAACGTCC-3'; antisense 5'-AAGTACCGTTGAGGCTCC-3'; 830 bp product. ICAM-1 sense: 5'-CTTGGATCGCTGCTTCAT-3'; antisense 5'-AGCGGAGCTCAGCACTA-3'; 592 bp product. As a probe of a non-promoter DNA, primers for a region upstream of the iNOS promoter were generated. Sense 5'-GTGTCACACCACAGAGCTGC-3'; antisense 5'-GTGTCTCTGCTCCTCCATCC-3'; 984 bp product. The PCR conditions were as follows: 5 μ L of 10X Taq buffer, 1.2-1.8 mM MgCl₂, 200 μ M deoxyribonucleotides, 0.6 μ M primer mix, 0.05 U Platinum Taq DNA polymerase and H₂O to a final volume of 50 μ L. PCR conditions were as follows: 94°C for 90 s; 35 cycles at 94°C for 30 s, 54-66°C (depending on primer set) for 30 s and 72°C for 60 s; final elongation at 72°C 10 min. Samples were run on a 1% agarose gel and bands, digitally imaged, analyzed with Image J software (NIH, ver. 1.22d; <http://rsb.info.nih.gov/ij/>), and the integrated intensity of bands was calculated. The average pixel intensity and number of pixels in a band were multiplied to determine the total signal intensity. The ratio of antibody bound DNA samples was divided by the input sample for each dilution. The ratios were averaged for each treatment condition, and indicate the relative presence of histones on specific DNA sequences.

DNAse I digestion and In situ Nick Translation (ISNT). After treatment of 6 wells per condition, cells in 96-well plates were fixed by addition of formaldehyde directly into the medium to a concentration of 1% for 10 min 37°C. Cells were washed three times with PBS and made permeable by incubation overnight in 70% ethanol at -20°C. Cells were washed three times with PBS at 4°C. The relative sensitivity of nuclear DNA to digestion with exogenous nucleases

was used to detect global alterations in chromatin structure (Hewish and Burgoyne, 1973; Hoyt et al., 1996a; Hoyt et al., 1996b). Cells were rinsed in ISNT Buffer (2.5 mM MgCl₂, 50 mM Tris (pH 7.8), 10 mM β-mercaptoethanol and 10 μg/ml bovine serum albumin) and then digested for 25 min at room temperature with 0 or 20 U DNase I/ml in ISNT Buffer. The cells were rinsed three times with PBS. DNA breaks were then labeled by ISNT with Digoxigenin-dUTP. (Hoyt et al., 1997). Cells were incubated at 37°C for 80 min with ISNT Buffer (2.5 mM MgCl₂, 50 mM Tris (pH 7.8), 10 mM β mercaptoethanol, 10 μg/ml bovine serum albumin) containing 16 μM each dGTP, dATP, and dCTP, 16 μM Digoxigenin-dUTP, and 2 U DNA polymerase I/ml. Labeling was stopped by rinsing with PBS. Wells were blocked with 10% goat serum/TTBS for 1 hr, incubated for 1 hr with a 1:1000 dilution of mouse anti-digoxigenin in 10% goat serum/TTBS, washed 3 times with TTBS and incubated for 1 hr with 1:1000 dilution of goat anti-mouse HRP antibody. Amplex red reagent and hydrogen peroxide were added to each well according to manufacturer's instructions (Molecular Probes, Eugene, OR). Fluorescence was detected in a fluorescent microplate reader with 562 nm excitation, 599 emission and a 590 nm cutoff. Relative fluorescent units (RFU) were obtained at 15 minutes in the linear phase of fluorescence. DNA content in each well was determined by addition of 25 ug/ml 33342 Hoechst with 355 nm excitation and 465 nm emission. RFU were normalized to DNA content in each well.

Statistical Testing. Data were analyzed by Student's *t* test or by analysis of variance (ANOVA) with Bonferroni correction for multiple comparisons (Snedecor, 1980).

Results

Previous studies demonstrated that engagement of $\beta 1$ integrins with antibody caused a global increase in sensitivity of MLEC DNA to digestion with nucleases (Jones et al., 2001). To determine the mechanisms underlying nuclease hypersensitivity, specific components of the chromatin architecture were probed for distinct post-translational modifications. Poly(ADP-ribosyl)ation and acetylation generally cause decondensation of chromatin, rendering DNA more susceptible to digestion with nucleases (Realini and Althaus, 1992; Simpson, 1978).

Linker histone H1 is the predominant histone modified with poly(ADP-ribose), which relaxes chromatin. Furthermore, a role for PARP-1 in integrin action was suggested by observations that integrin-engagement failed to inhibit drug-induced DNA breakage in PARP-1 knockout cells, and that knockouts were hypersensitive to DNase I (Huang et al., 2003; Jones et al., 2001). Therefore, we assessed poly(ADP-ribosyl)ation of histone H1 and its association with PARP-1 and DNA by immunoprecipitation of histone H1 from wildtype and PARP-1 knockout MLEC. PARP-1 co-immunoprecipitated with histone H1 in untreated wildtype cells, reflecting a basal association between the two proteins, and trichostatin A and integrin-engagement did not affect this interaction. Furthermore, poly(ADP-ribosyl)ation of PARP-1 and of histone H1 in H1 immunoprecipitates was unaffected by trichostatin A or integrin-engagement (not shown). Histone H1 levels in PARP-1 knockout MLEC were equal to those in wildtype cells and, as expected, no poly(ADP-ribosyl)ation or association of PARP-1 with histone H1 was detected in the knockouts (not shown). The results indicate that integrin-engagement and trichostatin A did not affect poly(ADP-ribosyl)ation of the 2 main nuclear substrates of PARP-1.

We next measured the effect of integrin-engagement on histone acetylation. Wild-type MLEC were treated with integrin antibody and proteins were extracted for western blotting. Figure 1a demonstrates a significant increase in acetyl-histone H3 in $\beta 1$ integrin antibody-treated MLEC.

The effect of raising histone acetylation with a broad-spectrum histone deacetylase inhibitor, trichostatin A, was compared with integrin-engagement. As expected, trichostatin A caused a concentration-dependent increase in global acetylation of histone H3 (Figure 1b). Trichostatin A also increased the sensitivity of nuclear DNA to digestion with DNase I (Figure 2).

Chromatin immunoprecipitation was used to measure local alterations in histone-DNA co-localization in live cells. We determined the effect of integrin-engagement on the level of acetyl-histone H3 at the ICAM-1, VCAM-1 and iNOS promoter DNA sequences, near the start codons of these genes where specific transcription factors are known to bind. Histone co-immunoprecipitation with a region 4763 base pairs 5' of the iNOS promoter sequence, which is characterized for a lack of consensus sites for transcription factors, was also measured. Integrin-engagement increased the co-immunoprecipitation of acetyl-histone H3 with ICAM-1 and VCAM-1 promoters, and with the sequence upstream of the iNOS promoter (Figure 3 a, b and c). There was no effect on acetyl-histone H3 co-immunoprecipitation with the iNOS promoter sequence (Figure 3d).

Since integrin-engagement increased global and local histone H3 acetylation, we next determined the effect of trichostatin A on acetyl-histone H3 chromatin immunoprecipitation. As seen with β 1-integrin-engagement, trichostatin A increased the level of acetyl-histone H3 co-immunoprecipitated with VCAM-1 and ICAM-1 promoters and with the iNOS upstream sequence (Figure 4 a, b, and c). Also as with integrin-engagement, acetyl-histone H3 co-immunoprecipitated with iNOS promoter DNA was not affected by trichostatin A (Figure 4d).

The effects of trichostatin A and integrin-engagement on association of linker histone H1 with DNA was determined since reduced association of histone H1 with DNA may render DNA susceptible to nuclease digestion (Hansen, 2002). The histone H1 content of MLEC, measured by western blotting, was not affected by β 1-integrin antibody or trichostatin A (not shown). Integrin-engagement decreased the level of linker histone H1 associated with the VCAM-1 and iNOS promoters (Figure 5). Trichostatin A treatment reduced the association of histone H1 with

the ICAM-1 and VCAM-1 promoters, and with the iNOS upstream sequence, but not with the iNOS promoter (Figure 6).

Acetyl-histone H3 levels were greatly elevated in PARP-1 knockout relative to wildtype MLEC (Figure 7). Furthermore, as with integrin-engagement and treatment of wildtype cells with trichostatin A, co-immunoprecipitation of acetyl-histone H3 with VCAM-1 and iNOS promoter DNA and with DNA 5' of the iNOS promoter was increased in knockouts (Figure 8 b, c, d). In contrast, co-immunoprecipitation of ICAM-1 promoter DNA was reduced in PARP-1 knockout cells (Figure 8a). As with integrin-engagement and trichostatin A treatment, the amount of histone H1 at the iNOS promoter was decreased (Figure 9). These data indicate that acetylation of the core histone H3 is increased in response to deletion of PARP-1, and that there were changes in histone-DNA co-immunoprecipitation that were generally similar, but not identical, to those caused by integrin-engagement or the histone deacetylase inhibitor.

Discussion

Previously we found that $\beta 1$ integrin-engagement increased the sensitivity of MLEC DNA to digestion by nucleases, indicating that chromatin structure is altered (Huang et al., 2003; Jones et al., 2001). Here we investigated the impact of integrin engagement on poly(ADP-ribosyl)ation and histone acetylation since both post-translational modifications regulate chromatin structure (Peterson and Cote, 2004).

Poly(ADP-ribosyl)ation of histones and other nuclear proteins dramatically increases negatively charged polymers of ADP-ribose in the vicinity of DNA breaks resulting in relaxation of chromatin structure (Perez-Lamigueiro and Alvarez-Gonzalez, 2004). This action of PARP-1 is thought to aid in the recruitment and access of DNA repair proteins to sites of DNA breaks (D'Amours et al., 1999; Parsons et al., 2005). Previously we found that integrin-mediated suppression of BLM- and LPS-induced DNA strand breakage was prevented in PARP-1 knockout MLEC (Huang et al., 2003; Jones et al., 2001). Therefore, we hypothesized that integrin-engagement might activate PARP-1 to generate polymers of ADP-ribose on nuclear proteins that would enhance nuclease sensitivity, recruit repair proteins, and ultimately suppress DNA damage. However, we found here that integrin engagement had no effect on poly(ADP-ribose) formation on the major PARP-1 targets, histone H1 and PARP-1. The requirement for PARP-1 in integrin-mediated suppression of drug-induced DNA breakage may be due to the direct role of PARP-1 protein in facilitating DNA repair rather than through modification of chromatin.

Acetylation of lysines neutralizes positive charge and reduces interaction of amino tails with negatively charged DNA (Hansen, 2002). In fact, raising acetylation with inhibitors of histone deacetylases causes nuclease hypersensitivity (Simpson, 1978). As expected, inhibition of histone deacetylases with trichostatin A in the present study increased the level of acetyl-histone H3 (Figure 1b) and enhanced nuclease sensitivity (Figure 2). While integrin-engagement did not affect poly(ADP-ribosyl)ation, it increased histone H3 acetylation (Figure

1a) and nuclease sensitivity (Jones et al., 2001). The results suggest that acetylation of histone H3 may contribute to the effect of integrin engagement on chromatin.

Interestingly, PARP-1 knockouts which are hypersensitive to nuclease digestion (Jones et al., 2001), were also highly acetylated on histone H3 (Figure 8). Therefore, acetylation may also contribute to chromatin alterations in these cells. However, deletion of PARP-1 may raise nuclease sensitivity independent of acetylation. In vitro degradation of an oligonucleotide substrate by cellular nucleases was increased in PARP-1-depleted and PARP-1 knockout cell extracts, suggesting that PARP-1 directly protects DNA (Parsons et al., 2005). PARP-1 may also indirectly protect DNA by recruiting DNA binding proteins such as NF κ B (Chang and Alvarez-Gonzalez, 2001), and by association with nucleosomes, which promotes compaction (Kim et al., 2004). Acetylation and the absence of PARP-1 molecules together may produce the nuclease hypersensitivity seen in the knockouts.

Increased histone H3 acetylation in integrin antibody-treated and PARP-1 knockout cells may result from activation of histone acetyl transferases and/or reduction or inhibition of histone deacetylases. With respect to PARP-1, fibroblasts from knockout embryos had decreased expression of a number of histone acetyl transferases, but their activity was not measured (Ota et al., 2003). The activities of histone acetyl transferases and deacetylases need to be assessed in PARP-1 knockout and integrin antibody-treated MLEC. Acetylation may also increase in response to other histone post-translational modifications, such as phosphorylation or ubiquitination, which can affect the susceptibility of histones to acetyl transferases and deacetylases (Berger, 2001).

Having assessed the global chromatin characteristics, we measured histone presence at promoter and non-promoter DNA to begin examining local variations in DNA-protein interactions in integrin antibody-, trichostatin A- treated and PARP-1 knockout MLEC. Chromatin immunoprecipitation revealed increased relative presence of acetyl-histone H3 at promoter and non-promoter DNA targets (Figures 3, 4, 8). Exceptions to this general trend at the ICAM

promoter in PARP-1 knockouts, and the iNOS promoter in trichostatin A- and integrin-antibody-treated MLEC, suggest that additional factors modulate the presence of acetyl-histone H3 at specific DNA targets. Nevertheless, increases in acetyl-histone H3 are consistent with global nuclease hypersensitivity in these experimental conditions.

Trichostatin A, β 1 integrin-engagement and PARP-1 knockout generally reduced the level of linker histone H1 associated at the promoter and non-promoter DNA targets (Figures 5, 6, and 9). As an exception, trichostatin A did not reduce histone H1 association with iNOS promoter DNA, suggesting that additional factors affect histone H1 association at particular DNA targets. In any case, reduction in histone H1-DNA association in treated and knockout MLEC is also consistent with global nuclease hypersensitivity.

This study focused on the chromatin structural alterations caused by integrin-engagement. The results suggest that acetylation of histone H3 may contribute to the opening of chromatin in response to integrin signals. In several other experimental systems, histone acetylation is associated with enhanced DNA repair (Bird et al., 2002; Hasan and Hottiger, 2002; Peterson and Cote, 2004; Ramanathan and Smerdon, 1989). Whether integrin-mediated acetylation of histone H3 inhibits drug-induced DNA damage or enhances repair remains to be determined.

In summary, integrin-engagement, trichostatin A, and PARP-1 knockout increased acetylation of histone H3 and caused nuclease hypersensitivity in MLEC. Consistent with these global effects, the level of acetyl-histone H3 present at several DNA targets was increased, while histone H1 association was generally reduced. The results suggest that integrin-engagement, and trichostatin A and PARP-1 deletion, regulate chromatin structure via core histone H3 acetylation and linker histone H1 dissociation.

Acknowledgments

We thank Csaba Szabo, Inotek Corporation, Beverly, MA for providing PARP-1 knockout mice.

The technical assistance of Rostislav I. Likhovvorik is also greatly appreciated.

References

- Ame JC, Spenlehauer C and de Murcia G (2004) The PARP superfamily. *Bioessays* **26**:882-93.
- Aplin AE, Howe A, Alahari SK and Juliano RL (1998) Signal transduction and signal modulation by cell adhesion receptors: the role of integrins, cadherins, immunoglobulin-cell adhesion molecules, and selectins. *Pharmacol Rev* **50**:197-263.
- Berger SL (2001) An embarrassment of niches: the many covalent modifications of histones in transcriptional regulation. *Oncogene* **20**:3007-13.
- Bird AW, Yu DY, Pray-Grant MG, Qiu Q, Harmon KE, Megee PC, Grant PA, Smith MM and Christman MF (2002) Acetylation of histone H4 by Esa1 is required for DNA double-strand break repair. *Nature* **419**:411-5.
- Buckley S, Driscoll B, Barsky L, Weinberg K, Anderson K and Warburton D (1999) ERK activation protects against DNA damage and apoptosis in hyperoxic rat AEC2. *Am J Physiol* **277**:L159-66.
- Chang WJ and Alvarez-Gonzalez R (2001) The sequence-specific DNA binding of NF-kappa B is reversibly regulated by the automodification reaction of poly (ADP-ribose) polymerase 1. *J Biol Chem* **276**:47664-70.
- D'Amours D, Desnoyers S, D'Silva I and Poirier GG (1999) Poly(ADP-ribosyl)ation reactions in the regulation of nuclear functions. *Biochem J* **342 (Pt 2)**:249-68.

- Hansen JC (2002) Conformational dynamics of the chromatin fiber in solution: determinants, mechanisms, and functions. *Annu Rev Biophys Biomol Struct* **31**:361-92.
- Hasan S and Hottiger MO (2002) Histone acetyl transferases: a role in DNA repair and DNA replication. *J Mol Med* **80**:463-74.
- Hazlehurst LA, Valkov N, Wisner L, Storey JA, Boulware D, Sullivan DM and Dalton WS (2001) Reduction in drug-induced DNA double-strand breaks associated with beta1 integrin-mediated adhesion correlates with drug resistance in U937 cells. *Blood* **98**:1897-903.
- Hewish DR and Burgoyne LA (1973) Chromatin sub-structure. The digestion of chromatin DNA at regularly spaced sites by a nuclear deoxyribonuclease. *Biochem Biophys Res Commun* **52**:504-10.
- Hoyt DG, Mannix RJ, Gerritsen ME, Watkins SC, Lazo JS and Pitt BR (1996a) Integrins inhibit LPS-induced DNA strand breakage in cultured lung endothelial cells. *Am J Physiol* **270**:L689-94.
- Hoyt DG, Rizzo M, Gerritsen ME, Pitt BR and Lazo JS (1997) Integrin activation protects pulmonary endothelial cells from the genotoxic effects of bleomycin. *Am J Physiol* **273**:L612-7.
- Hoyt DG, Rusnak JM, Mannix RJ, Modzelewski RA, Johnson CS and Lazo JS (1996b) Integrin activation suppresses etoposide-induced DNA strand breakage in cultured murine tumor-derived endothelial cells. *Cancer Res* **56**:4146-9.

- Huang H, McIntosh JL, Fang L, Szabo C and Hoyt DG (2003) Integrin-mediated suppression of endotoxin-induced DNA damage in lung endothelial cells is sensitive to poly(ADP-ribose) polymerase-1 gene deletion. *Int J Mol Med* **12**:533-40.
- Jones CB, McIntosh J, Huang H, Graytock A and Hoyt DG (2001) Regulation of bleomycin-induced DNA breakage and chromatin structure in lung endothelial cells by integrins and poly(ADP-ribose) polymerase. *Mol Pharmacol* **59**:69-75.
- Kim M, Mauro S, Gévry N, Lis J and Kraus W (2004) NAD⁺-Dependent Modulation of Chromatin Structure and Transcription by Nucleosome Binding Properties of PARP-1. *Cell* **119**:803-14.
- Meredith JE, Jr., Fazeli B and Schwartz MA (1993) The extracellular matrix as a cell survival factor. *Mol Biol Cell* **4**:953-61.
- Ota K, Kameoka M, Tanaka Y, Itaya A and Yoshihara K (2003) Expression of histone acetyltransferases was down-regulated in poly(ADP-ribose) polymerase-1-deficient murine cells. *Biochem Biophys Res Commun* **310**:312-7.
- Parsons JL, Dianova, II, Allinson SL and Dianov GL (2005) Poly(ADP-ribose) polymerase-1 protects excessive DNA strand breaks from deterioration during repair in human cell extracts. *Febs J* **272**:2012-21.
- Perez-Lamigueiro MA and Alvarez-Gonzalez R (2004) Polynucleosomal Synthesis of Poly(ADP-ribose) Causes Chromatin Unfolding as Determined by Micrococcal Nuclease Digestion. *Ann N Y Acad Sci* **1030**:593-598.

Peterson CL and Cote J (2004) Cellular machineries for chromosomal DNA repair. *Genes Dev* **18**:602-16.

Ramanathan B and Smerdon MJ (1989) Enhanced DNA repair synthesis in hyperacetylated nucleosomes. *J Biol Chem* **264**:11026-34.

Realini CA and Althaus FR (1992) Histone shuttling by poly(ADP-ribosylation). *J Biol Chem* **267**:18858-65.

Simpson RT (1978) Structure of chromatin containing extensively acetylated H3 and H4. *Cell* **13**:691-9.

Snedecor GaCW (1980) *Statistical Methods*. Iowa State University Press, Ames.

Footnotes

This work was supported by HL68054 from the National Heart, Lung, and Blood Institute. Its contents are solely the responsibility of the authors and do not necessarily represent the official views of the National Heart, Lung, and Blood Institute or NIH.

Figure Legends

Figure 1. Effect of integrin-engagement and trichostatin A (TSA) on acetylation of core histones.

A. MLEC were treated with 0 or 1 $\mu\text{g/ml}$ $\beta 1$ integrin antibody for 1 h and then with goat-anti rat IgG (2 $\mu\text{g/ml}$ final concentration) for 4 h. Proteins were extracted and processed for western blotting. **B.** MLEC were treated with 0, 0.01, 0.1 and 1 μM trichostatin A (TSA) for 24 h. Proteins were extracted and processed for western blotting. Acetyl-histone H3 was measured by western blotting and analyzed densitometrically. Blots were also probed with total histone H3 antibody, analyzed and used to normalize acetyl-histone H3 levels. Bars represent the mean + S.E. of 4 independent cultures per treatment group. *, $p < 0.05$ for comparison with 0 $\mu\text{g/ml}$ $\beta 1$ integrin antibody. ***, $p < 0.001$ for comparison with 0 μM trichostatin A (TSA). Inset for **A** is a representative image of acetyl-histone H3 in 0 or 1 $\mu\text{g/ml}$ $\beta 1$ integrin antibody treatments. Inset for **B** is a representative image of acetyl-histone H3 in 0, 0.01, 0.1 or 1 μM trichostatin A (TSA) treatment.

Figure 2. Effect of trichostatin A (TSA) on DNase I sensitivity. MLEC were treated with 0, 0.01 and 0.1 μM trichostatin A (TSA) for 24 h. Cells were processed and digested with 20 U/ml DNase I for 25 min and breaks in DNA were labeled by ISNT. Bars represent the mean of fluorescent intensity + S.E. of the difference for 6 wells for each experimental group. * $p < 0.05$ for comparison between 0 and 0.1 μM trichostatin A (TSA) in DNase treated wells.

Figure 3. Effect of integrin-engagement on acetylation of histone H3 at local genomic sites using chromatin immunoprecipitation (ChIP). MLEC were treated with 0 (clear bars) or 1 $\mu\text{g/ml}$ $\beta 1$ integrin antibody for 1 h (solid bars), and then with goat-anti rat IgG (2 $\mu\text{g/ml}$ final concentration) for 4 h. Cells were treated with formaldehyde to cross-link proteins, proteins immunoprecipitated with 10 μg anti-acetyl-histone H3 antibody, reverse cross-linked and

associated DNA was isolated and amplified using PCR. Bars represent the average + S.E. of Bound (*B*) over Input (*I*) levels analyzed densitometrically from 1% agarose gels from 4 independent cultures per treatment group with at least 9 independent PCR reactions per treatment. The *B* level represents PCR product from samples immunoprecipitated with antibody with no antibody blank subtracted. *I* is the PCR product from 1% of the sample before immunoprecipitation used to normalize for treatment changes in total DNA content. A dilution series of template DNA was used to ensure PCR product formation increased linearly with template concentration. **p*<0.05, ****p*<0.0001 for comparison between 0 and 1 µg/ml β1 integrin antibody. **A** represents acetyl-histone H3 co-immunoprecipitated with the intercellular adhesion molecule-1 (ICAM-1) promoter. **B** represents acetyl-histone H3 co-immunoprecipitated with the vascular adhesion molecule-1 (VCAM-1) promoter. **C**, acetyl-histone H3 co-immunoprecipitated with sequences upstream of the inducible nitric oxide synthase (iNOS) promoter. **D**, acetyl-histone H3 co-immunoprecipitated with the iNOS promoter.

Figure 4. Effect of trichostatin A (TSA) on acetylation of histone H3 at local genomic sites using ChIP. MLEC were treated with 0 (clear bars) or 0.1 µM trichostatin A (TSA) (solid bars) for 24 h. Cells were processed as in figure 3. **A**, represents acetyl-histone H3 co-immunoprecipitated with the ICAM-1 promoter. **B**, represents acetyl-histone H3 co-immunoprecipitated with the VCAM-1 promoter. **C**, acetyl-histone H3 co-immunoprecipitated with sequences upstream of the iNOS promoter. **D**, acetyl-histone H3 co-immunoprecipitated with the iNOS promoter. **p*<0.05, ***p*<0.001 for comparison between 0 and 0.1 µM trichostatin A (TSA).

Figure 5. Effect of integrin-engagement on association of Histone H1 at local genomic sites using ChIP. MLEC were treated with 0 (clear bars) or 1 µg/ml β1 integrin antibody (solid bars)

for 1 h and then with goat-anti rat IgG (2 µg/ml final concentration) for 4 h. Cells were processed as in figure 3, except 10 µg Histone H1 antibody was used for immunoprecipitation. **A**, represents histone H1 associated with the VCAM-1 promoter. **B**, represents histone H1 associated with the iNOS promoter. ** $p < 0.01$ for comparison between 0 and 1 µg/ml β1 integrin antibody.

Figure 6. Effect of trichostatin A (TSA) on association of Histone H1 at local genomic sites using ChIP. MLEC were treated with 0 (clear bars) 0.1 µM trichostatin A (TSA) (solid bars) for 24 h. Cells were processed as in figure 5. **A**, represents histone H1 associated with the ICAM-1 promoter. **B**, represents histone H1 associated with the VCAM-1 promoter. **C**, histone H1 associated with sequences upstream of the iNOS promoter. **D**, histone H1 associated with the iNOS promoter. ** $p < 0.005$, * $p < 0.05$ for comparison between 0 and 0.1 µM trichostatin A (TSA).

Figure 7. Acetyl-Histone H3 protein levels in wild-type (PARP +/+) and PARP-1 knockout (PARP -/-) MLEC. PARP +/+ (clear bar) and PARP -/- (solid bar) MLEC proteins were extracted and processed for western blotting. Acetyl-histone H3 was measured by western blotting and analyzed densitometrically. Blots were also probed with total histone H3 antibody, analyzed and used to normalize acetyl-histone H3 levels. Bars represent the mean + S.E. of 4 independent cultures per treatment group. ***, $p < 0.0002$ for comparison with PARP +/+.

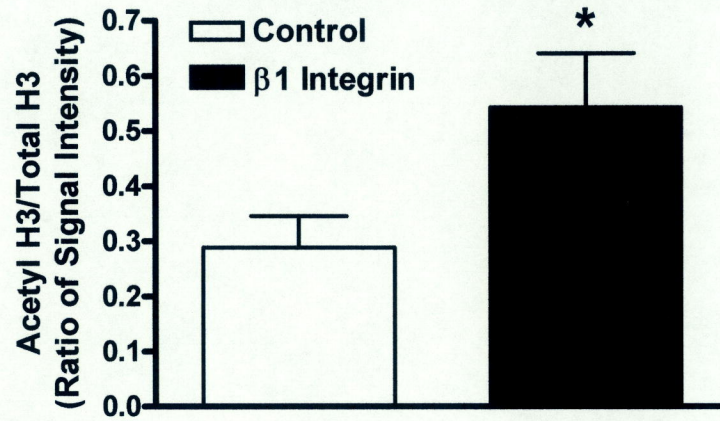
Figure 8. Effect of PARP-1 on acetyl-Histone H3 immunoprecipitation at local genomic sites using ChIP. PARP +/+ (clear bar) and PARP -/- (solid bar) MLEC were processed as in figure 3. **A**, represents acetyl-histone H3 co-immunoprecipitated with the ICAM-1 promoter. **B**, represents acetyl-histone H3 co-immunoprecipitated with the VCAM-1 promoter. **C**, acetyl-

histone H3 co-immunoprecipitated with sequences upstream of iNOS promoter. **D**, acetyl-histone H3 co-immunoprecipitated with the iNOS promoter. * $p < 0.05$, ** $p < 0.001$ and $p < 0.0001$ for comparison between PARP +/+ and PARP -/-.

Figure 9. Effect of PARP-1 on Histone H1 association at iNOS promoter using ChIP. PARP +/+ (clear bar) and PARP -/- (solid bar) MLEC were processed as in figure 5. Bars represent relative histone H1 associated with the iNOS promoter. * $p < 0.05$, for comparison between PARP +/+ and PARP -/-.

Fig. 1.

A.



B.

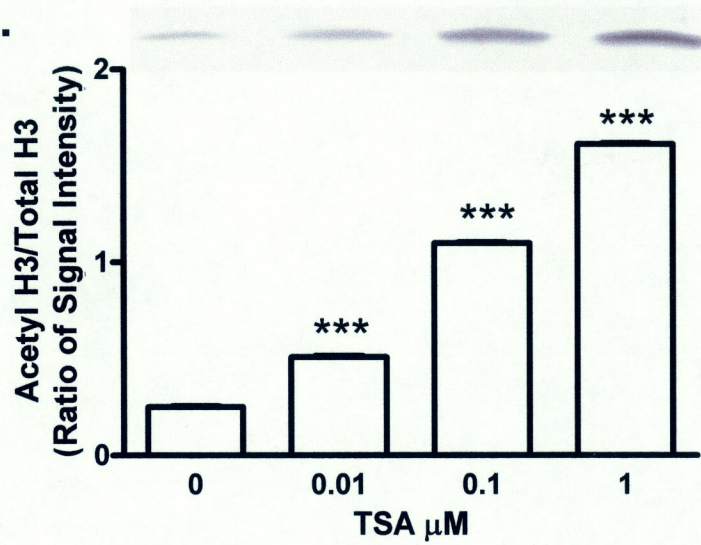


Fig. 2.

MOL 10876R

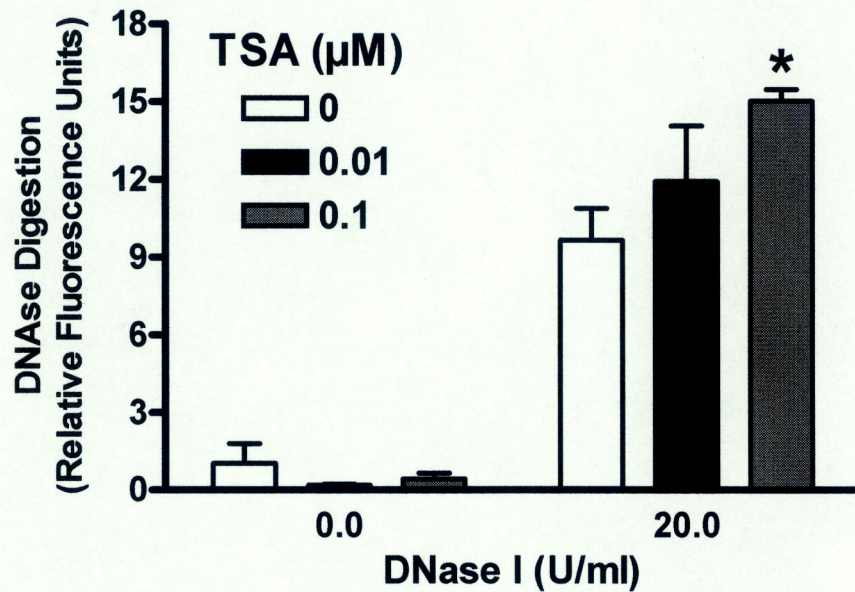
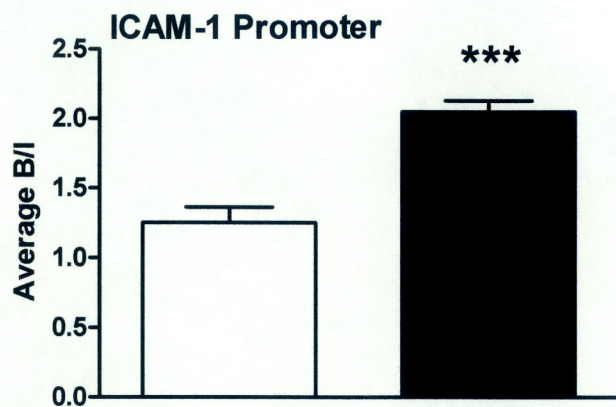
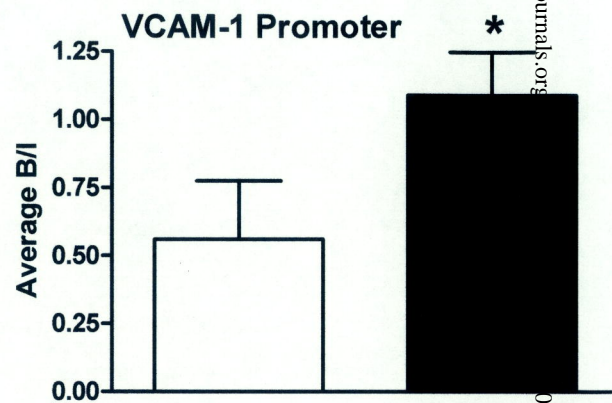


Fig. 3.

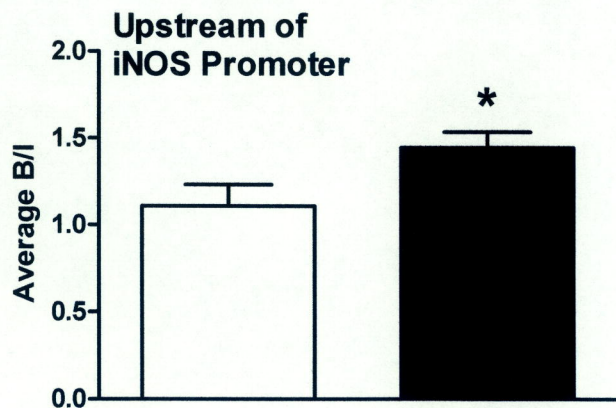
A.



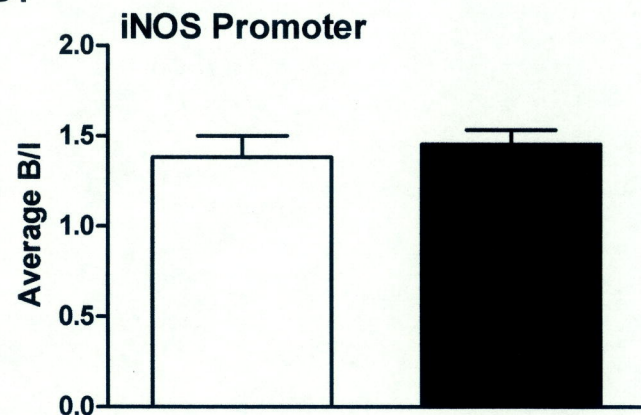
B.



C.



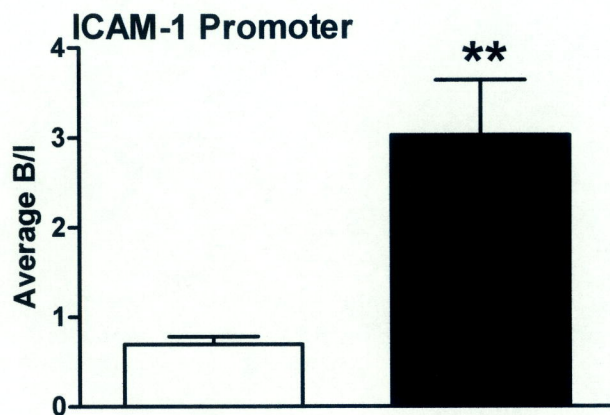
D.



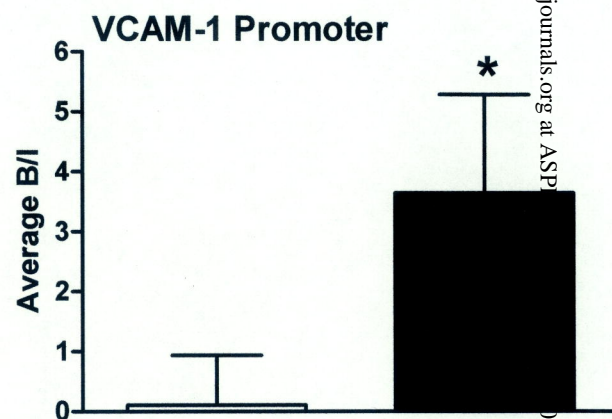
MOL 10816R

Fig. 4.

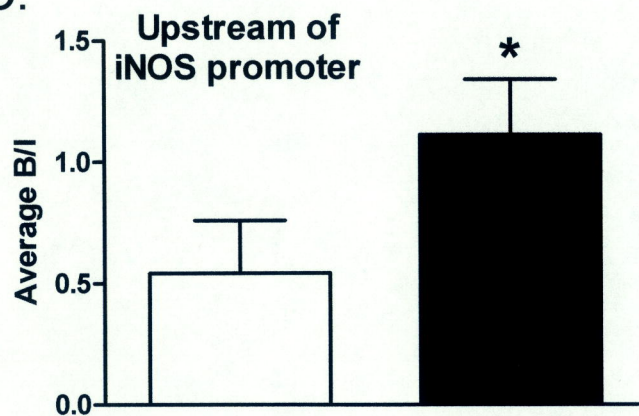
A.



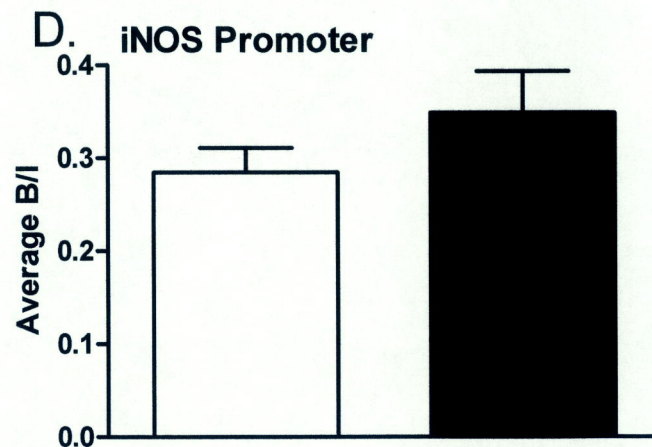
B.



C.



D.

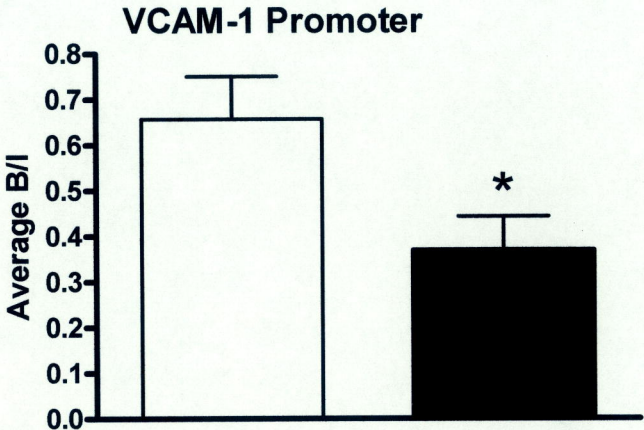


MOL 10876R

Fig. 5.

MOL 10876R

A.



B.

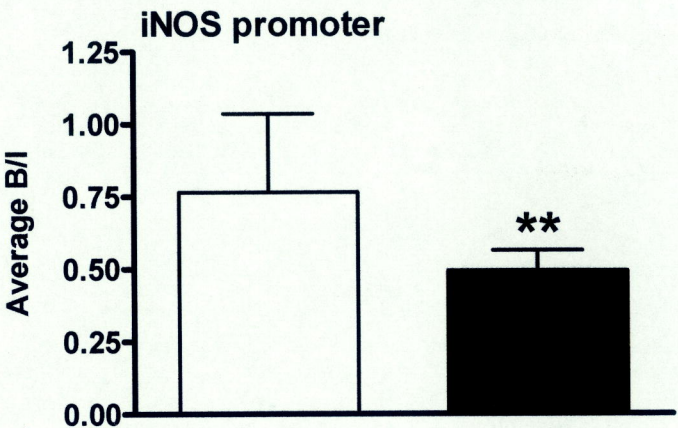
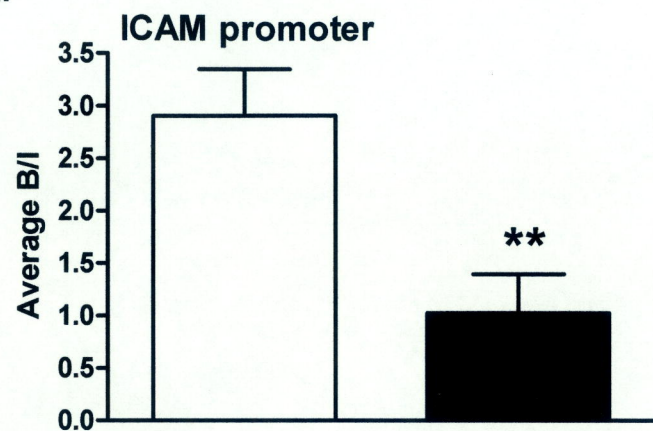
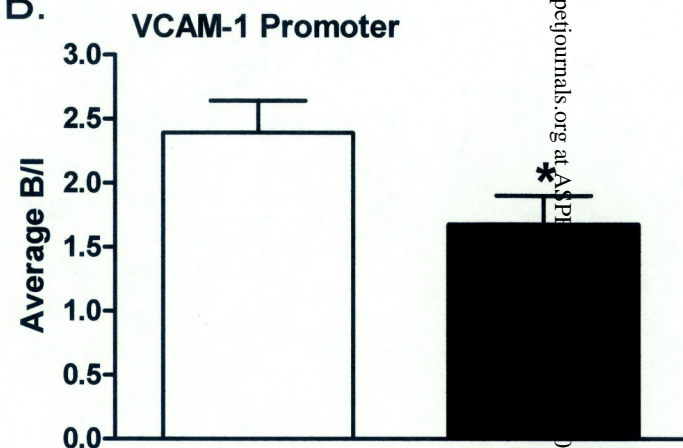


Fig. 6.

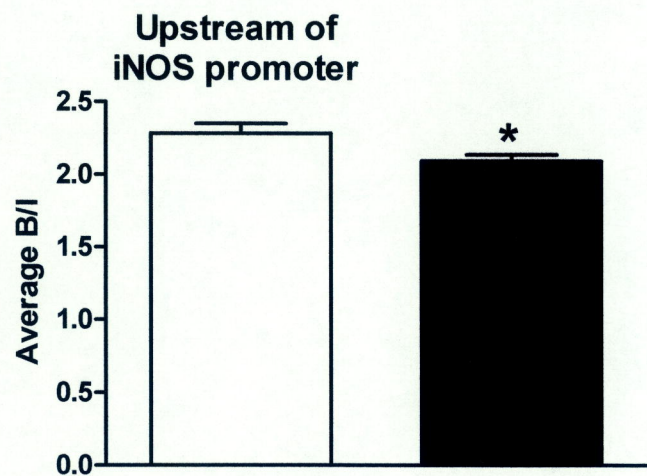
A.



B.



C.



D.

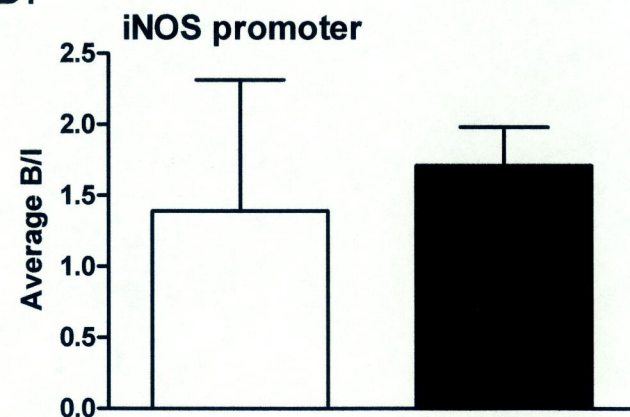


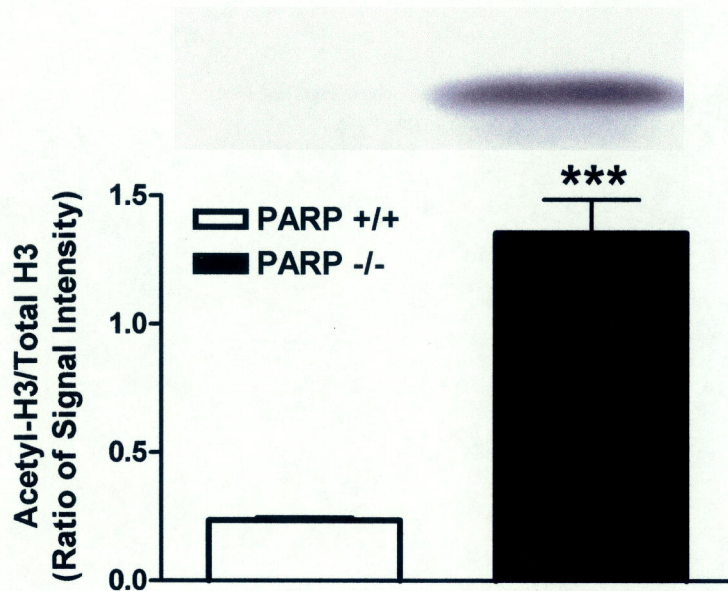
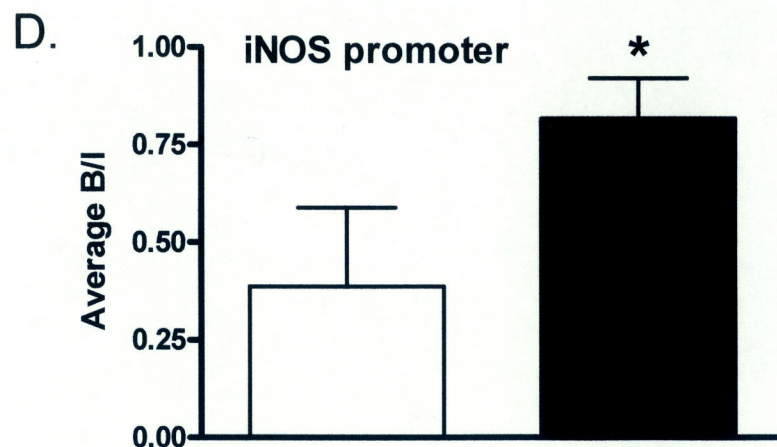
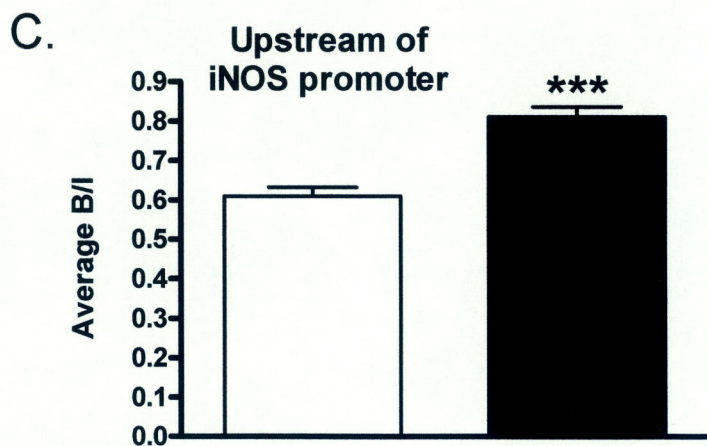
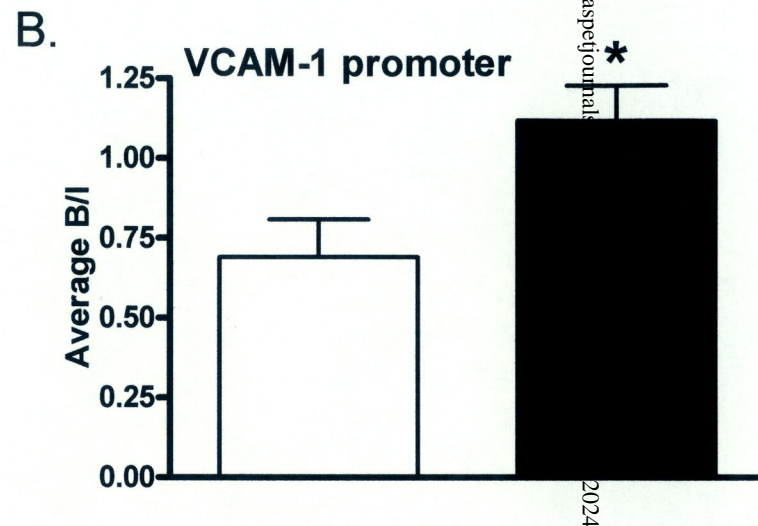
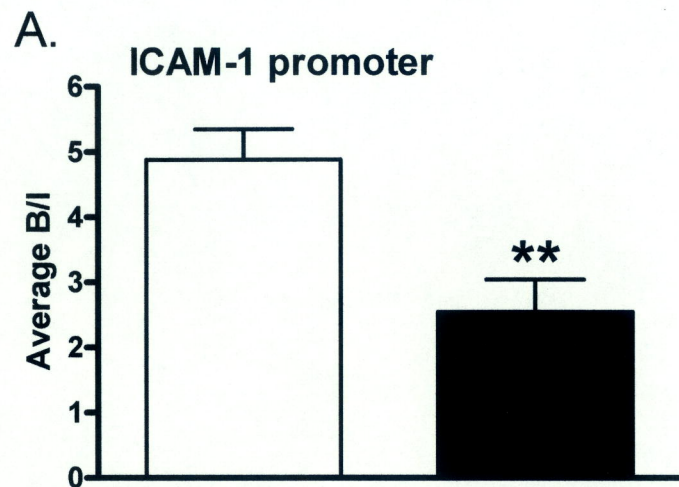
Fig. 7.

Fig. 8.



MO 10876R

Fig. 9.

MOL 10876R

